Sheffield Hallam University

Multimodal analytical approach applied to whisky labels for authenticity determination

TIBLJAS, Veronika, FRANCESE, Simona <http://orcid.org/0000-0002-1381-1262>, CLARK, Jef, GOODALL, Ian, BIRCH, Frazer and BRADSHAW, Robert <http://orcid.org/0000-0003-1533-2166>

Available from Sheffield Hallam University Research Archive (SHURA) at:

https://shura.shu.ac.uk/36715/

This document is the Published Version [VoR]

Citation:

TIBLJAS, Veronika, FRANCESE, Simona, CLARK, Jef, GOODALL, Ian, BIRCH, Frazer and BRADSHAW, Robert (2025). Multimodal analytical approach applied to whisky labels for authenticity determination. Forensic Chemistry, 46: 100709. [Article]

Copyright and re-use policy

See http://shura.shu.ac.uk/information.html

Sheffield Hallam University Research Archive
http://shura.shu.ac.uk

Forensic Chemistry 46 (2025) 100709

Contents lists available at ScienceDirect

Forensic Chemistry

journal homepage: www.sciencedirect.com/journal/forensic-chemistry

Multimodal analytical approach applied to whisky labels for authenticity determination

Veronika Tibljas [a], Simona Francese [a], Jef Clark [a], Ian Goodall [b], Frazer Birch [c], Robert Bradshaw [a,*]

[a] Centre for Mass Spectrometry Imaging, Biomolecular Research Centre, City Campus, Sheffield Hallam University, Howard Street, Sheffield S11WB, United Kingdom
[b] The Scotch Whisky Research Institute, The Robertson Trust Building, Research Avenue North, Riccarton Edinburgh, EH144AP, United Kingdom
[c] Edrington, Great Western Road, Glasgow G15 6RW, United Kingdom

ARTICLE INFO

Keywords:
Counterfeit
Whisky
MALDI MS
DESI MS
Raman spectroscopy

ABSTRACT

Alcohol counterfeiting presents a significant global challenge, posing serious health risks and economic losses. Whisky, a leading UK commodity export, is a common target for counterfeiting due to its high value and global demand. Counterfeit detection of this and similar products most often involves analysis of the liquid content, which requires opening of the products. This study explores a multimodal analytical workflow for whisky label authentication, integrating Raman spectroscopy, desorption electrospray ionisation mass spectrometry imaging (DESI MSI), and matrix-assisted laser desorption/ionisation mass spectrometry imaging (MALDI MSI). Raman spectroscopy provides a rapid, non-invasive method that can be used as initial testing. The subsequent application of DESI MSI and MALDI MSI in sequence maximises the chemical intelligence obtained from the labels and strengthens confidence in counterfeit identification, with additional potential presented for quality control (QC) in label printing and design.

1. Introduction

Whisky is made from three main ingredients: water, cereals and yeast. These ingredients undergo various processes, including fermentation, distillation and maturation to create the finished product [1]. Depending on the nature of the cereal, production methods and country of origin these products can be categorised into various classes e.g. Single Malt Scotch Whisky, Blended Scotch Whisky, Irish Pot Still Whiskey, Bourbon etc. According to the Food and Drink Federation, whisky is the number one export commodity in the UK [2], and is a common target for counterfeiting due to its high value and global demand. In 2017, a high-profile case of whisky fraud made headlines when a bottle of Macallan 1878 at the *Waldhaus Hotel am See* in St Moritz, Switzerland, was exposed as counterfeit [3]. Researchers from the University of Oxford conducted carbon dating tests on the liquid content, which indicated a 95 % likelihood that the spirit was produced between 1970 and 1972 [4]. The incident gained international attention after a tourist paid 9999 CHF (approximately £7700 or $10,050) for a single dram from this supposedly ultra-rare Scotch whisky. It is not known if the bottle and labelling itself were fake. However, this scenario exemplifies a broader issue of alcohol counterfeiting that calls for increased attention. A news article on counterfeit alcohol by Food Standards Scotland (2021) [5] highlighted the threat of widespread national trade in counterfeit products; as consuming these cheap alternatives could pose a significant health risk (if the content is unknown and not sufficiently tested for public consumption) and, in the worst cases, could be fatal.

Traditionally, whisky analysis has been primarily performed on the liquid content using various analytical techniques. Some of these include high resolution gas chromatography-olfactometry (HRGC-O) [6], aroma extract dilution analysis [6], thermal desorption high resolution gas chromatography–mass spectrometry (TD-HRGC–MS) [6], gas chromatography mass spectrometry (GC–MS) [7–13], gas chromatography with flame ionisation detection (GC-FID) [14], ^{1}H NMR spectroscopy [15] and ultra-high performance liquid chromatography (UHPLC) [16]. The choice of analytical techniques depends on the target molecules; for example high performance liquid chromatography (HPLC) is commonly applied for sugar analysis whereas GC is used for volatiles such as alcohols. Liquid content analysis of these products remains a crucial tool for quality control (QC), ensuring that the quantity of the components

* Corresponding author.
E-mail address: r.bradshaw@shu.ac.uk (R. Bradshaw).

https://doi.org/10.1016/j.forc.2025.100709
Received 22 July 2025; Received in revised form 24 October 2025; Accepted 26 October 2025
Available online 28 October 2025
2468-1709/© 2025 The Authors. Published by Elsevier B.V. This is an open access article under the CC BY license (http://creativecommons.org/licenses/by/4.0/).

responsible for the unique aroma and flavour is preserved. Aside from QC, the composition of the liquid can also be used for determining authenticity of these products, safeguarding consumers. For example, authenticity of the whisky products has been verified using 1H NMR [17], UV-Vis [18], inductively coupled plasma mass spectrometry (ICP-MS) [19], inductively coupled plasma optical emission spectrometry (ICP-OES) [19], cold vapor-atomic absorption (CVAAS) [19], two-dimensional gas chromatography coupled to mass spectrometry (GC X GC–MS) [20] and desorption atmospheric pressure chemical ionisation mass spectrometry (DAPCI-MS) [21]. The main limitation of these methodologies for authenticity testing is the requirement to open the bottle or pierce the cork to extract liquid samples.

To protect the consumers and preserve the integrity of these products, it would be advantageous to develop more rapid and less destructive techniques for identifying counterfeits. Recent advancements in analytical technologies make it possible to analyse product labels, enabling faster detection of counterfeit items by examining the chemistry of inks and the substrates onto which they are deposited. Raman spectroscopy is often used in forensic examinations, due to its fast and non-destructive nature, with limited/no sample preparation requirements. Previously, it has been successfully applied to questioned documents analysis [22], crossing ink lines [23], discrimination of pen inks [24–27], banknotes and driver licences [28]. Asri et al. (2021) demonstrated that Raman spectroscopy combined with chemometrics can be utilised to categorise documents printed with various sources (laser, inkjet and photocopier) [29]. They analysed 387 printed samples and successfully assigned 15 unknown printed samples to their source based on molecular composition. For example, carbon black was identified in the laser and inkjet printed samples, whilst pigment violet 19 was found in photocopier samples. Spectroscopic methods also allow the analysis of bottled liquids with the possibility of "through the container" analysis such as glass, providing a non-invasive and non-destructive method preserving the integrity of the products. Most recent work, where Raman was used on ethanol and illicit alcohols (methanol and isopropanol) in beverages [30] showed some limitations, including scattering from the glass and the restriction posed by the colour of the liquid (dark-coloured spirits exhibited a suppressed signal due to laser absorption).

Developments in ink analysis in recent years have shown clear distinction not only between different types of inks (printed, ballpoint, stamp etc) [31–34] but also the ability to differentiate between the brands of the same type of ink [35–38]. It has been shown that inks consist of many chemical components, including pigments, dyes, solvents and additives and, depending on the brand, they will exhibit differentiable chemical profiles. For example, Sun et al. (2016) quantitatively assigned triphenylmethane basic dyes detected in twenty ballpoint pen inks, including Victoria Blue B, Victoria Blue R, Basic Blue 7 and Ethyl Violet [39]. Furthermore, research conducted by Bello de Carvalho et al. (2018) demonstrated correlations between various pen brands based on the composition of the ink dyes, including acid yellow 3, Victoria blue 4R, Basic violet 4, and Basic blue 9 [40]. Our group applied mass spectrometry to differentiate seven different ballpoint pens, and also provide information of the relative time of deposition of pen strokes [41]. The same technique could be applied to the analysis of the product labels, on the premise that genuine samples have chemically distinguishable labels to the counterfeits, allowing differentiation between a genuine and counterfeit commodity. Similarly, the same hypothesis can be applied to the substrate (e.g. paper) that labels are printed on.

Mass spectrometry, a widely used analytical technique for ink analysis, has previously proven successful in distinguishing between different ink types and brands. Sun et al. (2016) [37] discriminated 18 blue ballpoint inks using GC-MS, thin layer chromatography (TLC), liquid chromatography tandem mass spectrometry (LC-MS/MS) and the video spectral comparator (VSC), a conventional optical technique used in questioned document analysis. They report that none of the methods alone distinguished all 18 inks and therefore suggest that in order to achieve effective discrimination of entries made by the same ink type, the examination should involve analytical methods targeting additional properties of inks (optical features, volatile solvents and dyes).

In order to overcome these challenges, our group has developed a multimodal approach, progressing in order of increasing destructiveness (Raman spectroscopy, followed by DESI MSI, and then MALDI MSI) to maximise the intelligence recovered from a single sample. The approach was applied to the analysis of whisky labels to test for authenticity, and also to explore the possibility of the proposed methodology to serve as QC for label printing. This approach would mitigate issues with opening of the products, offering a rapid and simple method of detection whilst allowing the liquid content to remain uncompromised. The use of a portable Raman spectrometer for initial sample interrogation also presents the possibility for analysis at the point of seizure, therefore streamlining forensic protocols ahead of the more confirmatory mass spectrometry analyses. To the best of the authors' knowledge, this study is the first to apply multiple analytical techniques to product labels for authenticity testing.

2. Experimental

2.1. Chemicals

Trifluoroacetic acid (TFA) and α-cyano-4-hydroxycinnamic acid (CHCA) were purchased from Sigma Aldrich (Poole, UK). Formic acid and HPLC grade acetone, methanol (MeOH) and acetonitrile (ACN) were obtained from Fisher Scientific (Loughborough UK). Double-sided conductive carbon tape was purchased from TAAB (Aldermaston, UK). MiliQ water was obtained from the inhouse system.

2.2. Whisky label samples

Whisky labels were generously provided by the Scotch Whisky Research Institute (SWRI) (Edinburgh, UK) and Edrington (Glasgow, UK). These labels were not attached to whisky bottles and therefore extraction prior to analysis was not required. A mock counterfeit label was produced inhouse using a high-quality scanner and laser printer *bizhub C659* Konica Minolta (Tokyo, Japan) with a pigment-based toner.

2.3. Instrumentation

Raman spectroscopy analysis was performed on BWTek Portable iRaman Plus source (Metrohm group, Herisau, Switzerland), equipped with a 785 nm laser and 3.72 cm^{-1} measured resolution. The full laser power measured at the excitation port is 488 mW. Sampling areas included the analysis of the substrate, black ink and gold ink (Fig. 1). The instrument was operated in microscope mode (x20 magnification) with 10 s integration time, average spectrum number set to 1 and laser power optimised for each region. Specifically, laser power for the black region was set to 2 % (9.76 mW), gold region to 7 % (34.16 mW) and substrate to 10 % (48.8 mW). The different coloured regions of the samples are shown in Fig. 1. Laser powers were optimised to prevent thermal degradation of the sample.

MALDI-MS and DESI-MS analyses in both profiling and imaging mode were conducted on a SELECT SERIES Multi Reflecting Time-of-Flight (MRT) mass spectrometer (Waters Corporation, Wilmslow, UK). The MRT was operated in "MRT mode" (which allows for MS resolution of 200,000 FWHM), with the laser set to 1 kHz. Both instruments were run with 0.2 s scan time, 50 μm pixel size and raster rate of 250 μm s^{-1}. Continuous Lockmass Correction (CLMC) was implemented during the acquisition for both instruments during analysis. For MALDI-MS in positive ion mode, CLMC was applied on the matrix peak at *m/z* 212.0324 and for DESI-MS in negative ion mode, CLMC was applied on Leucine Enkephalin peak at *m/z* 554.2615. The quad profile was set to Automatic for data acquisition in a full mass range (0–2400 m/z). The

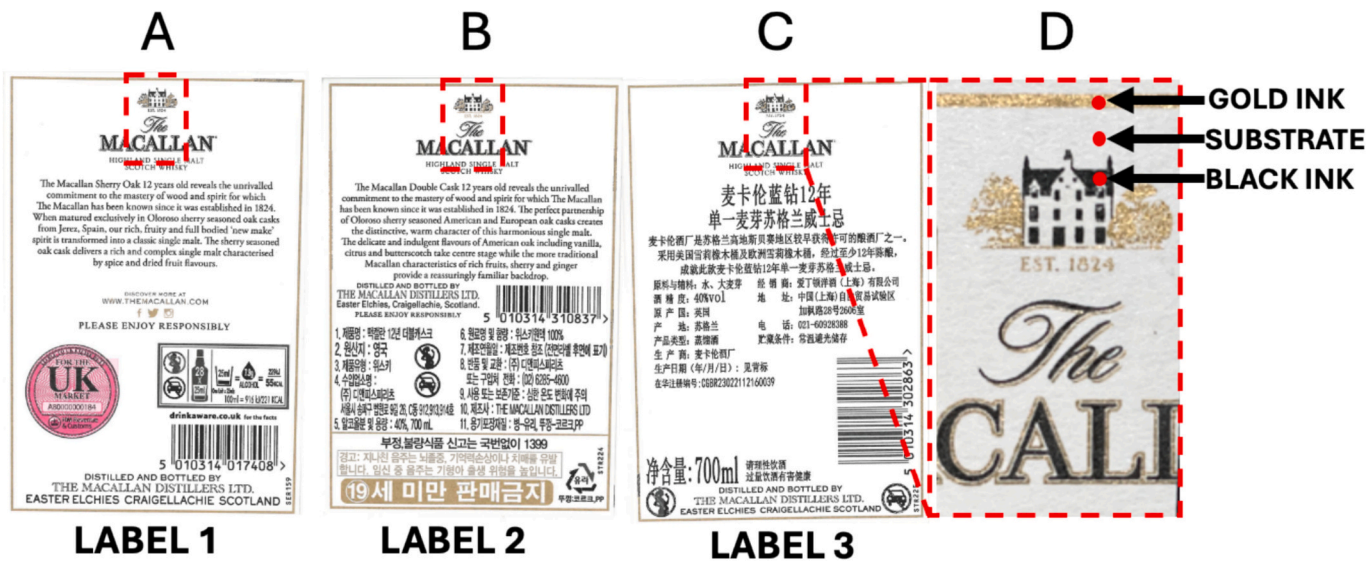

Fig. 1. Three genuine Macallan whisky labels: a) Label 1, b) Label 2 and c) Label 3. The sampling areas for mass spectrometry imaging are highlighted with red dashed outlines, with red circles in panel d) indicating the sampling areas for Raman analysis. (For interpretation of the references to colour in this figure legend, the reader is referred to the web version of this article.)

data acquisition and processing were conducted using MassLynx version 4.2, HDI version 1.8, (Waters Corporation, Wilmslow, UK). Images were normalised by the total ion count (TIC) and the contrast and intensity were set to maximise quality of each image. Mean prediction error for the DESI-MS and MALDI-MS analysis following calibration for both instruments was <0.2 ppm. Matrix spraying for MALDI-MSI analysis was performed on HTX M3+ Sprayer™ (HTX Imaging, North Carolina, USA).

2.4. Sample preparation

The labels were cut to size and secured to a single glass slide using double sided-carbon tape prior to analysis. The sample contained Label 1, Label 2, Label 3 which are genuine Macallan whisky labels sourced from different production batches and intended for different global destinations. Label 4 was a counterfeit label that was produced inhouse using a high-quality scanner and printer. Each sample underwent initial Raman analysis, followed by DESI-MSI analysis in negative ion mode, and then MALDI-MSI in positive ion mode. No sample preparation was required for Raman spectroscopy or DESI-MSI.

For DESI-MSI analysis, a solvent mixture of 95:5 MeOH:H_2O spiked with 100 pg μL^{-1} of Leu-enkephalin was employed, sprayed at a flow rate of 2 $\mu L min^{-1}$. Data acquisition was performed in negative ion mode, with a capillary voltage set at 0.5 kV, cone voltage at 40 V, source temperature of 120 °C and the heated transfer line set to 30 °C.

Prior to MALDI-MSI analysis, 5 mg/ml of α-CHCA matrix in 70:30 MeOH:0.5 %TFA (aq) matrix was spray-coated the using HTX M3+ Sprayer™ (HTX Imaging, North Carolina, USA) using a solvent flow rate of 100 $\mu L min^{-1}$ and a N_2 pressure of 8 psi, in 8 layers, at a velocity of 1300 mm/min.

2.5. Statistical analysis

Mass spectra from regions of interest (ROI) were exported for each label using the (MVA) tool in HDI 1.7. Subsequently, the data was imported into MetaboAnalyst 6.0 for further analysis. Raman data, in .csv format, was extracted from the instrument, baseline corrected in Python and imported into Metaboanalyst 6.0 for analysis. One-factor statistical analysis was conducted, with Pareto scaling applied to all datasets. Principal component analysis (PCA) was applied to evaluate the underlying patterns in the data.

3. Results and discussion

3.1. Raman spectroscopy

In the first stage of the proposed multimodal workflow three genuine Macallan whisky labels (1–3) and a mock counterfeit label (4) were subjected to Raman analysis. The acquired Raman spectra are shown in Fig. 2 (a-c). The analysis involved three sampling areas for each label: (a) the substrate (which in this set of samples is paper), (b) the black ink region, and (c) the gold line region (the sampling areas are highlighted with red circles in the optical image) (Fig. 2 (d)). Triplicate measurements were taken from each region and a representative spectrum for these three regions is shown for all labels (1–4).

Raman analysis of the substrates of all labels (1–4) shows a peak at ~1100 cm^{-1} associated with $CaCO_3$ used for treatment of the paper [29,42,43]. Additionally, the observed differences at ~500 cm^{-1} in Raman spectra of genuine vs counterfeit samples are likely to be due to the formation of dialkylsulfide bonds (C-S-S-C), that occur during the chemical pulping of straw and wood used to produce the paper pulp [44,45]. These signals are visible for genuine samples (Labels 1–3) showing 3 peaks in this region 250–750 - cm^{-1}, whereas the same area for Label 4 is showing no/weak signals in this region. These results suggest that the genuine whisky labels were printed on a type of paper with a higher cellulose fibre content.

Raman analysis of the gold ink region revealed unique peaks in the region of 1400–1600 cm^{-1} for the counterfeit label (label 4), often found in several yellow pigments [46]. Conversely, gold ink of genuine labels (1–3) showed the presence of two peaks in the region 2000–3000 cm^{-1}, the identity of which remain unknown. Importantly, this data provides a positive indication that Raman spectroscopy can provide initial differentiation between genuine and fake whisky labels through analysis of multiple regions.

The analysis of black ink regions produced more peak-rich spectra, as expected, given that black inks typically consist of more complex molecules. It has previously been shown that laser black printout, carbon black pigment and toner samples show the presence of a peak at ~1550 cm^{-1}, corresponding to a C═O stretch in carbonyl or OH-C=O in carboxylic acid [27,29]. All labels (1–4) show peaks in region. However, distinctive peaks differentiate genuine labels from the counterfeit, suggesting that different black inks were used for printing. Furthermore, the counterfeit label displayed a unique peak at around 750 cm^{-1}, also

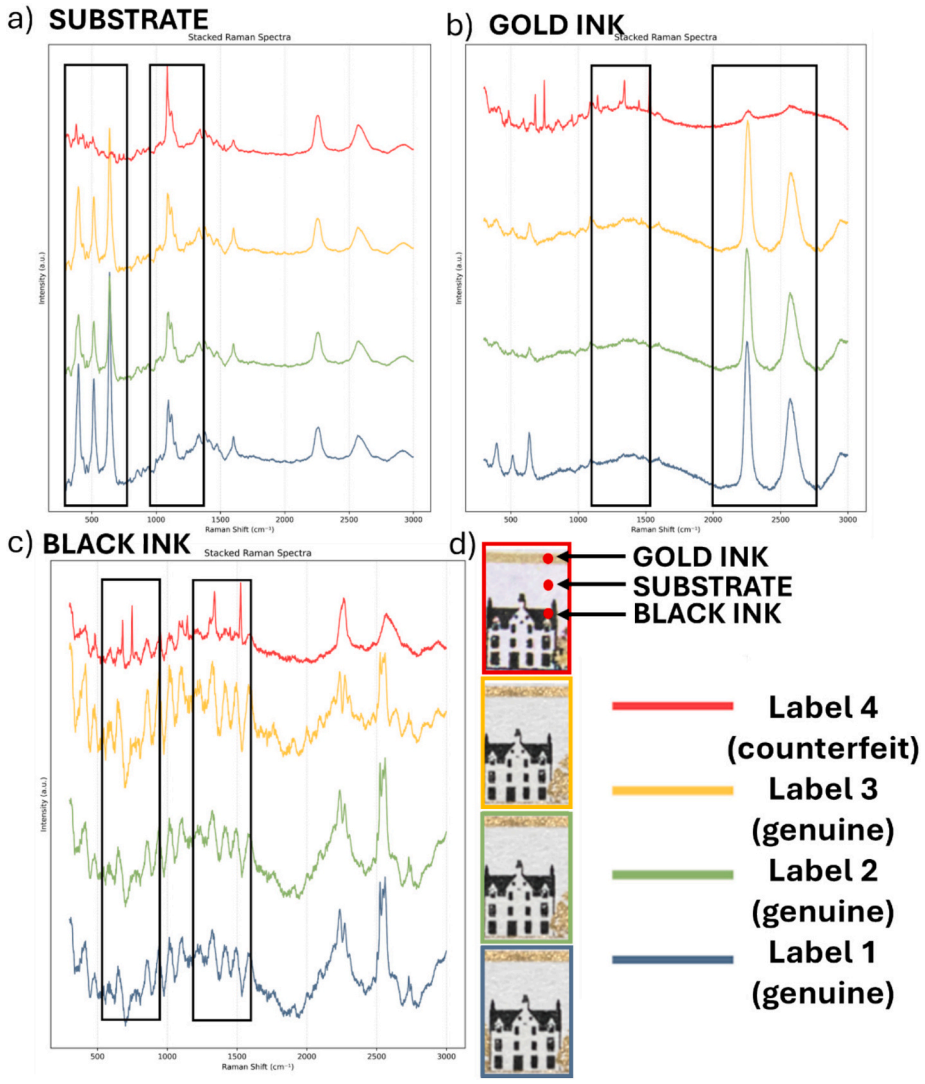

Fig. 2. Raman spectra collected from different regions of Labels 1–4: a) substrate, b) gold ink and c) black ink. (d) shows the analysed regions within the optical images. (For interpretation of the references to colour in this figure legend, the reader is referred to the web version of this article.)

observed by Heudt et al. (2012) [43] in black inkjet printouts, although they did not speculate on its origin.

Following Raman analysis, the triplicate data points for each of the three regions: substrate, gold ink, and black ink were analysed using the statistical tool MetaboAnalyst 6.0 (Fig. 3 (a-c)). PCA loadings plots were obtained for the respective regions across all whisky labels (1–4).

3.2. *Substrates*

The PCA scores plot reveals that measurements from the paper

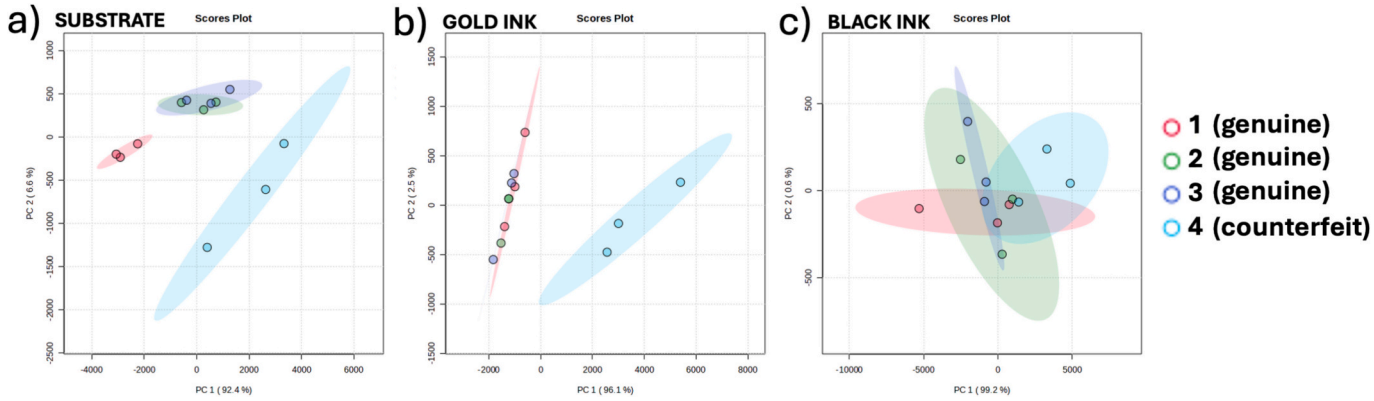

Fig. 3. PCA scores plot following Raman analysis in triplicates for: a) substrates, b) gold ink and c) black ink regions for labels 1–4. (For interpretation of the references to colour in this figure legend, the reader is referred to the web version of this article.)

substrates show an overlap of data points from genuine labels 2 and 3. They are distinct from labels 1 (genuine) and 4 (counterfeit), which are clustered separately, as evidenced by the strong influence of PC1 (92.6 %). It's important to note that all genuine labels fall within the same quadrant. It has been suggested by the producers that variation observed among the genuine examples could potentially be due to differences in the primers applied to the paper, though further work is necessary to confirm this. The data variability for the genuine labels is lower than that of the counterfeit label.

3.3. Gold ink

The PCA scores plot of data from the Gold Ink regions shows a clear distinction between the genuine labels (1–3) and the counterfeit (4), with PC1 accounting for 96.1 % of the variance. Once again, the counterfeit sample exhibits greater variability among the triplicates taken from gold ink region compared to the genuine samples, suggesting that the genuine samples exhibit more uniform printing when compared to the counterfeits.

3.4. Black ink

The PCA scores plot from the Raman analysis of black ink regions in Labels 1–4 shows the technique's limitations in (statistically) distinguishing the genuine labels from the counterfeit. This may be due to several factors, with a major contributor likely to be the complexity of the spectra from the black ink regions. However, the successful results obtained from the other regions of the labels highlights the usefulness of the methodology in the initial stages of counterfeit identification.

Ultimately, in this first step of the multimodal workflow, Raman analysis of whisky labels proved an effective, rapid, and non-invasive technique for verifying authenticity, suggesting counterfeit samples, and therefore highlights its beneficial use for initial testing. However, the methodology has limitations—for instance, in this study, some label regions, such as the gold ink, provided much more certain differentiation between genuine and counterfeit labels compared to the substrates and black inks. The presented results further support the need for a holistic approach to analysis. The generation of an in-house proprietary Raman database would allow not only counterfeit detection but also the possibility for QC (characterising the expected variation within genuine labels within and between batches). Modification of the chemical composition of genuine labels to incorporate a chemical marker could increase the confidence in authenticity determination, and indeed this methodology has been utilised elsewhere [47]. Where this presumptive test does not lead to a definitive answer, further confirmatory testing is needed, which could be achieved by mass spectrometry to offer specific molecular-level chemical information.

3.5. DESI MSI

Since DESI MSI has previously proven successful in differentiating inks by detecting characteristic chemical constituents [41], it was applied in negative ion mode to Labels 1–4, following Raman analysis, to explore the potential of this technique in providing confirmatory information assisting in counterfeit detection. In all instances, any successful identity of ions contained within the genuine exhibits has been omitted to preserve brand integrity. Fig. 4 (a) reveals the spatial distribution of a selection of ions present in genuine labels only (*m/z* 684.8932, *m/z* 330.9108, *m/z* 232.7637). On the other hand, spatial distribution of ions at *m/z* 555.2648 and *m/z* 367.2850 can be used to differentiate the counterfeit sample (Fig. 4 a). Fig. 4 (b) illustrates the sampling process for subsequent statistical analysis through the extraction of spectra from regions of interest (ROIs) from both the genuine and counterfeit samples, highlighted in different coloured squares. These ROIs were subjected to PCA and the obtained scores plot is shown in Fig. 4 (c), whereby a clear differentiation between genuine and counterfeit samples can be seen with the PC1 accounting for 82.4 %.

This technique provides spatially resolved molecular information, allowing for the generation of images that display distinct chemical profiles of genuine whisky labels (1–3) when compared to the counterfeit sample (4). The DESI MS molecular images at *m/z* 684.8932, *m/z* 330.9108, *m/z* 232.7637 (Fig. 4 (a)) show that these ions are only present in the genuine labels (1–3) and not in the counterfeit sample (4). As shown in Fig. S2, representative DESI-MSI spectra from the ROIs

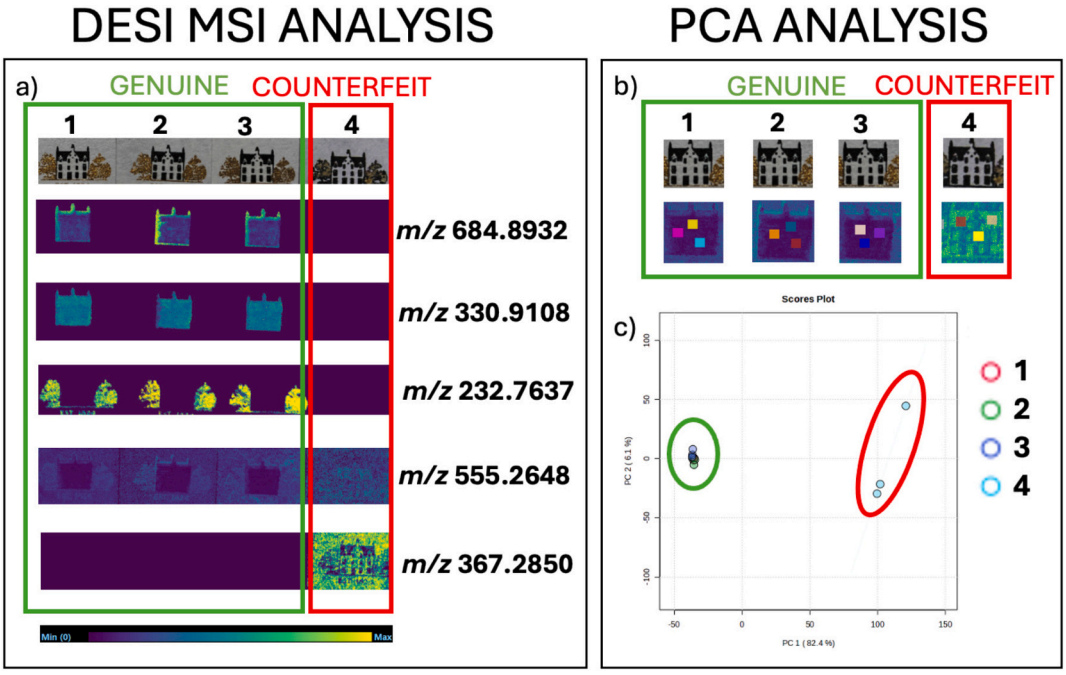

Fig. 4. DESI MSI analysis of genuine and counterfeit whisky labels, showing a) DESI MSI molecular images of ions *m/z* 684.8932, *m/z* 330.9108, *m/z* 232.7637, *m/z* 555.2648 and *m/z* 367.2850 across all Labels (1–4) showing differentiation between the genuine and counterfeit samples, b) ROIs extracted for statistical analysis and c) the PCA scores plot.

taken from the black and gold region confirm that ions at *m/z* 232.7637 and *m/z* 330.9108 are characteristic of genuine labels (1–3), whereas these ions are not detected in the counterfeit sample (4). These ions outline the areas of the black and gold regions of the genuine labels (1–3) and share similar signal intensity within the genuine labels, indicating consistency in the abundance of these molecules. It is important to emphasise that these labels are not from the same batch, showing that this consistency could be attributed to similarities in the printing process between different versions of the same label. These labels were printed within a period of 2 days and were stored under the same conditions prior to analysis which also accounts for the consistency in chemical composition. Previous groups have investigated the effect of storage condition on ink composition in so-called "ageing studies" and therefore future work will focus on how different environmental conditions (temperature, humidity and light) may impact the chemical profiles of genuine labels, an important consideration in maintaining quality of the product. The ion at *m/z* 684.8932 reveals an increase in signal intensity on the top and left sides of the house outlines in all three genuine labels (1–3), with some variation in the signal intensity. These differences could be attributed to the manufacturing process, suggesting that some labels have a greater amount of deposited material. This was not an isolated case, and other ions also showed slight differences in signal intensity between genuine labels (data not shown). Further work is necessary to identify these ions, which, for these product labels, can serve as valuable information from a QC perspective.

To gain a better understanding of the salient features in the data collected following DESI MSI, PCA analysis was performed by extraction of the three ROIs per feature (indicated by the different coloured squares) from each label (Fig. 4 (b)). The PCA scores plot (Fig. 4 (c)) reveals a clear distinction between the genuine and counterfeit samples represented by a PC1 of 82.4 %. ROIs extracted from the genuine whisky label demonstrate minimal variability, whereas the counterfeit sample shows greater inconsistency. These results, which align with the data acquired from Raman spectroscopy, may be attributed to the higher printing quality of genuine labels compared to that of the counterfeit label.

Although DESI MSI detected ions from the substrate of the counterfeit sample at *m/z* 555.2648 and *m/z* 367.2850 (Fig. 4 (a)), it showed limitations in detecting ions derived from the ink within the counterfeit sample. This could be due to the chemistry of the ink (whereby the molecular content may not be amenable to DESI MSI in negative ion mode), interaction of the ink components with the paper used for the counterfeit sample or the printing process employed. For example, inkjet printers use nozzles to spray liquid ink, which is expected to form a layered deposit on the surface, whereas laser printers use toner, a powdered pigment that bonds with the paper when heated [48]. It is hypothesised that this hinders the desorption of molecules contained within the ink from the surface of the sample when employing the minimally destructive DESI approach.

3.6. MALDI MSI

Following DESI MSI, the same samples underwent MALDI MSI analysis as the final step of the multimodal workflow. This technique requires sample preparation consisting of matrix deposition prior to analysis. Our group has successfully used MALDI MSI in positive ion mode in a recent casework example (data not shown due to confidentiality) and has shown its effectiveness to detect various dyes in ballpoint pen inks within this multimodal workflow [41].

Fig. 5 (a) reveals the spatial distribution of a selection of ions present only in genuine (*m/z* 695.1265, *m/z* 279.0939, *m/z* 443.0133) or counterfeit labels (*m/z* 445.0392 and *m/z* 861.0717). MALDI MSI analysis revealed ions derived from the black ink within the counterfeit sample which were not present in the genuine labels. The same statistical analysis was applied to MALDI dataset with ROIs extracted from both genuine and counterfeit samples. The PCA loadings plot (Fig. 5 (b)) shows a representative ion at *m/z* 279.0939 for genuine samples versus an ion representative of the counterfeit sample at *m/z* 445.0392. Specifically, the PCA scores plot (Fig. 5 (c)) shows a clear differentiation between genuine and counterfeit samples, with a PC1 of 91.2 % which is superior to the statistical differentiation achieved following DESI MSI.

Analysis of the samples using MALDI MSI yielded unique ions for both genuine and counterfeit labels. For example, the spatial distribution of the ions at *m/z* 695.1265, *m/z* 279.0939 and *m/z* 443.0133 (Fig. 5 (a)) is observed in the regions of the genuine labels only. As illustrated in Fig. S3, MALDI-MSI spectra acquired from the black region confirm a clear distinction between genuine and counterfeit labels: the ion at *m/z* 695.1265 is unique to genuine labels (1–3), whereas the ion at *m/z* 445.0133 is detected only in the counterfeit sample (4). Similarly to DESI MSI, ions within the house region display the same signal intensity

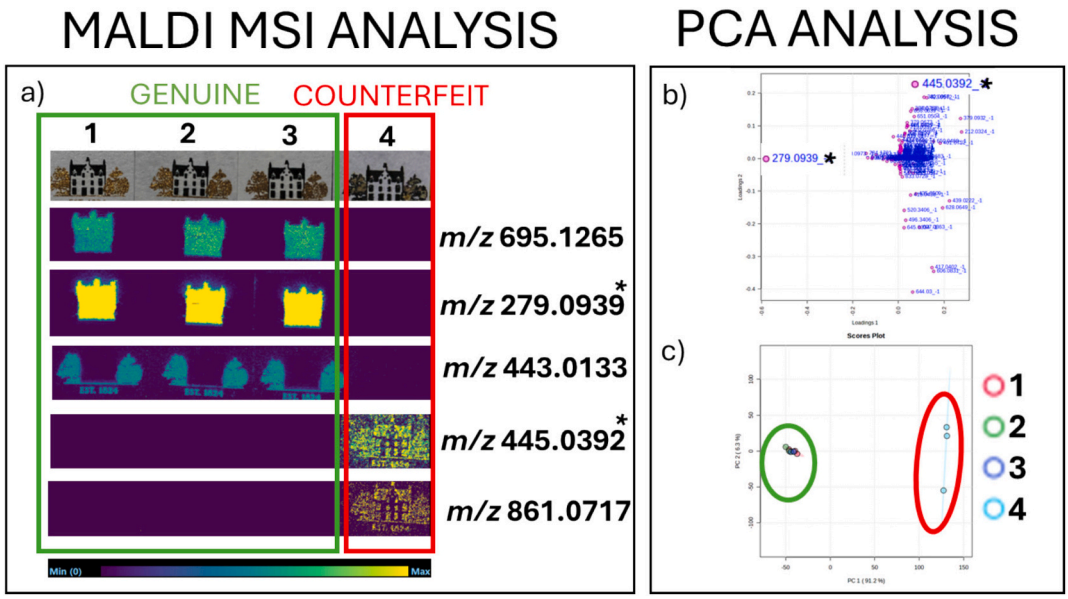

Fig. 5. MALDI MSI analysis of genuine and counterfeit whisky labels, showing a) MALDI MSI molecular images of ions *m/z* 695.1265, *m/z* 279.0939, *m/z* 443.0133, *m/z* 445.0392 and *m/z* 861.0717 showing differentiating ions between the genuine and counterfeit samples, b) PCA loadings plot and c) PCA scores plot.

across the three genuine labels (1–3). The ions at *m/z* 445.0392 and *m/z* 861.0717 are constituents of black ink used to print the counterfeit label. In contrast to the genuine labels, which show a uniform signal across the entire house region, these ions are more localised to the areas where black ink was deposited. It is hypothesised that this is due to the presence of a protective coating in this region of the genuine labels, which the manufacturers have confirmed is applied to reduce damage to the product. This prevents extraction of analytes contained within the ink, which was also observed with the data obtained from DESI MSI. This finding could also be relevant to different regions of the label and could potentially provide invaluable information for counterfeit detection. PCA analysis of the extracted spectra (Fig. 5 (c-d)) acquired using MALDI MSI further validated the previous results obtained with DESI MSI. The loadings plot (Fig. 5 (c)), is essential for interpreting the underlying structure of the data. For example, the ion at *m/z* 279.0939 is exclusive to the genuine samples. In contrast, the ion at m/z 445.0392 is unique to the counterfeit sample, both have been highlighted with an Asterix within the figure. The scores plot (Fig. 5 (d)) shows differentiation between the genuine and the counterfeit by a PC1 of 91.2 %. Similarly to DESI MSI experiment, the ROIs extracted from the house region of the counterfeit label show greater variability between the extracted spectra, certainly a consequence of the lack of uniformity in the signal intensity of different ions located within this region.

To maximise the intelligence recovered from the dataset, PCA analysis was performed on ROIs extracted from the substrate (paper) regions following both DESI MSI and MALDI MSI. The experiments reveal contrasting outcomes as unlike the observations from the house regions, the genuine labels display greater variance between the triplicates (Fig. 6). Similarly to what was observed in the Raman spectroscopy data, label 1 appears to be grouped separately from labels 2 and 3, suggesting some subtle difference between the genuine samples. As previously noted, this difference could be attributed to the use of a different primer, and has been confirmed as a potential difference between the samples by the producers.

Finally, the examination of matrix peaks provides insights into permeability of substrates on which the labels are printed. A representative example of a matrix peak can be seen in Fig. S1, at *m/z* 212.0324 (0 ppm). The ion at *m/z* 212.0324 represents a sodiated CHCA ion $[M + Na]^+$ which is displaying higher intensity signal within the counterfeit label in comparison to the genuine samples. This is likely a result of the genuine labels being printed on substrates which have different physical/chemical properties to that of the counterfeit. Furthermore, there appears to be less matrix coverage on the tree and house features of the genuine labels in comparison to the counterfeit sample, which could offer additional intelligence in this type of analysis. Again, this correlates to the previous data, and information provided by the producers, regarding the protective coating which is applied to this region to prevent damage.

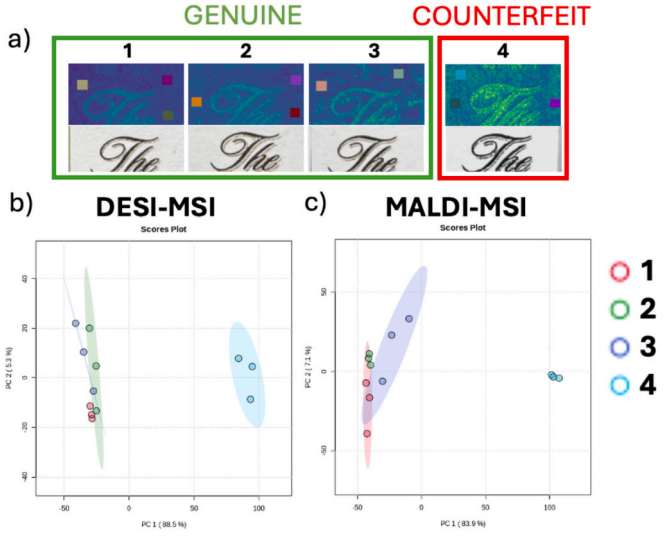

Fig. 6. DESI MSI and MALDI MSI analysis of the substrate (paper) region of genuine and counterfeit whisky labels, showing a) ROI extraction process for the triplicates taken from three genuine labels (1–3) and a counterfeit (4), b) PCA scores plot following DESI MSI and c) PCA scores plot following MALDI MSI.

The comparative assessment of different analytical methodologies underscores the advantage of employing MALDI MSI following DESI MSI in instances where DESI MSI does not yield a definitive result. While Raman-DESI MSI may be sufficient in some cases, this study highlights the importance of the full multimodal workflow, particularly when DESI MSI does not provide complete ink composition data. In this context, the combination of Raman and MALDI MSI may also be considered as an alternative workflow, although the MALDI MSI technique is more destructive, necessitating the deposition of a MALDI matrix prior to analysis, and is therefore reserved for the final stage of the proposed workflow. Indeed, the "harder" nature of MALDI technique enables more efficient extraction and ionisation of a broader range of analytes when compared to DESI which are more limited in the molecules they ionise [49]. Within this workflow, MALDI MSI enhances the amount of intelligence recovered from the sample, strengthening the ability to distinguish genuine labels from counterfeits with greater confidence.

To the best of the authors' knowledge, this study represents the first instance whereby different analytical techniques have been applied to product labels for authenticity testing. It highlights that spectroscopic and mass spectrometric techniques can assist in counterfeit detection and interestingly, their potential role in QC for product labels. It highlights the importance of maximising intelligence recovered from the samples through a multimodal workflow applied in order of increasing destructiveness and how the different analytical techniques can extract key chemical and physical information from different features of product labels.

4. Conclusion

This study highlights the applicability of different analytical techniques (in a multimodal analytical workflow) for whisky label authentication. Raman spectroscopy provides an effective initial method for authenticity testing, offering a non-invasive and rapid approach. However, its limitations in differentiating black regions can lead to inconclusive results and may necessitate further confirmatory analysis. DESI MSI successfully identified unique ions corresponding to features of the genuine labels but exhibited limitations in extraction ions derived from ink within the counterfeit labels. MALDI MSI addressed this issue by detecting ions specific to the counterfeit ink, likely due to the better analyte extraction capabilities. Despite MALDI MSI being destructive due to an additional sample preparation step, its application at the final stage of the workflow strengthens the overall analytical approach, enhancing confidence in distinguishing genuine labels from counterfeits. It is important to note that this proof-of-concept methodology would be feasible in cases in which the product labels were counterfeited, but not in instances where genuine bottles have been refilled.

Interestingly, both mass spectrometry techniques showed great potential for quality control (QC) in label printing by identifying variations in the chemical profiles of specific molecules within genuine samples. This intelligence could allow for improvements to be made in the manufacturing process. Further research is required to identify these molecules and evaluate their response to different environmental conditions, including temperature, light, and humidity to allow for the quality to be maintained following different storage conditions of the product.

CRediT authorship contribution statement

Veronika Tibljas: Conceptualization, Data curation, Formal analysis, Investigation, Methodology, Writing – original draft, Writing – review & editing. **Simona Francese:** Funding acquisition, Project administration, Supervision, Writing – review & editing. **Jennifer Clark:** Formal analysis, Writing – review & editing. **Ian Goodall:** Conceptualization, Project administration, Writing – review & editing. **Frazer Birch:** Conceptualization, Writing – review & editing. **Robert Bradshaw:** Conceptualization, Data curation, Formal analysis, Funding acquisition, Investigation, Methodology, Project administration, Resources, Supervision, Visualization, Writing – original draft, Writing – review & editing.

Declaration of competing interest

The authors declare that they have no known competing financial interests or personal relationships that could have appeared to influence the work reported in this paper.

Appendix A. Supplementary data

Supplementary data to this article can be found online at https://doi.org/10.1016/j.forc.2025.100709.

Data availability

The data that has been used is confidential.

References

[1] J.R. Piggott, in: A. Pandey, M.Á. Sanromán, G. Du, C.R. Soccol, C. Dussap (Eds.), In Current Developments in Biotechnology and Bioengineering, Elsevier, 2017, pp. 435–450.
[2] Food and Drink Federation, Trade Snapshot Q3, 2024 www.fdf.org.uk, https://www.fdf.org.uk/globalassets/resources/publications/reports/trade-reports/fdf-q3-trade-snapshot-2024.pdf , 2024.
[3] C. Mercer, Rare Scotch whisky at eight thousand pounds-a-dram is fake, Decanter, https://www.decanter.com/wine-news/fake-macallan-1878-scotch-whisky-379267-379267/, 2017.
[4] BBC, World's Most Expensive Dram of Scotch Was a Fake, https://www.bbc.co.uk/news/uk-scotland-scotland-business-41695774, 2017.
[5] Food Standards Scotland, Counterfeit Alcohol Can Seriously Damage Your Health, Warn Standards Agencies, https://www.foodstandards.gov.scot/news-and-alerts/counterfeit-alcohol-can-seriously-damage-your-health-warn-standards-agencies, 2021.
[6] L. Poisson, P. Schieberle, J. Agric. Food Chem. 56 (2008) 5813–5819, https://doi.org/10.1021/jf800382m.
[7] M. Lehtonen, Chromatographia 16 (1982) 201–203, https://doi.org/10.1007/BF02258900.
[8] A. Wanikawa, K. Hosoi, I. Takise, T. Kato, J. Inst. Brew. 106 (2000) 39–44, https://doi.org/10.1002/j.2050-0416.2000.tb00038.x.
[9] R.I. Aylott, A.S. McNeish, D.A. Walker, J. Inst. Brew. 93 (1987) 382–386, https://doi.org/10.1002/j.2050-0416.1987.tb04521.x.
[10] L.K. Ng, P. Lafontaine, J. Harnois, J. Chromatogr. A 873 (2000) 29–38, https://doi.org/10.1016/s0021-9673(99)01100-0.
[11] D. González-Arjona, G. López-Pérez, V. González-Gallero, A.G. González, J. Agric. Food Chem. 54 (2006) 1982–1989, https://doi.org/10.1021/jf0517389.
[12] A. Wanikawa, K. Hosoi, T. Kato, K. Nakagawa, Flavour, Fragr. J. 17 (2002) 207–211, https://doi.org/10.1002/ffj.1073.
[13] E. Campo, J. Cacho, V. Ferreira, J. Chromatogr. A 1140 (2007) 180–188, https://doi.org/10.1016/j.chroma.2006.11.036.
[14] Lehtonen, J. Pekka, A. LaDena A. Keller, T. Eero, Z Lebensm Unters Forsch A, 1999, https://doi.org/10.1007/s002170050439.
[15] M. Stockwell, I. Goodall, D. Uhrín, Analytical Sci. Adv. 1 (2020) 132, https://doi.org/10.1002/ansa.202000063.
[16] M. Picard, C. Oulieu, M. Nonier, N. Vivas, N. Vivas, J. Inst. Brew. 129 (2023) 62–79, https://doi.org/10.58430/jib.v129i1.8.
[17] T. Kuballa, T. Hausler, A.O. Okaru, M. Neufeld, K.O. Abuga, I.O. Kibwage, J. Rehm, B. Luy, S.G. Walch, D.W. Lachenmeier, Food Chem. 245 (2018) 112–118, https://doi.org/10.1016/j.foodchem.2017.10.065.
[18] A.R. Martins, M. Talhavini, M.L. Vieira, J.J. Zacca, J.W.B. Braga, Food Chem. 229 (2017) 142–151, https://doi.org/10.1016/j.foodchem.2017.02.024.
[19] M. Gajek, A. Pawlaczyk, K. Jóźwik, M.I. Szynkowska-Jóźwik, Foods 11 (2022) 1616, 10.3390/foods11111616 (DOI:10.3390/foods11111616).
[20] A. Ferracane, N. Manousi, P.Q. Tranchida, G.A. Zachariadis, L. Mondello, E. Rosenberg, J. Chromatogr. A 1676 (2022) 463241, https://doi.org/10.1016/j.chroma.2022.463241.
[21] B.L. Smith, D.M. Hughes, A. Badu-Tawiah, R. Eccles, I. Goodall, S. Maher, Sci. Rep. 9 (2019) 7994, https://doi.org/10.1038/s41598-019-44456-0.
[22] C.A. Teixeira, R.J. Poppi, Microchem. J. 144 (2018) 411, https://doi.org/10.1016/j.microc.2018.10.002.
[23] S.I. Sharaa, A.A.A. El-Magd, A.A. Bakr, Y.M. Moustafa, I.M.A. El-Aziz, Dyes Pigments 163 (2018) 393, https://doi.org/10.1016/j.dyepig.2018.12.016.
[24] S. Liu, J. Feng, J. Lv, W. Zhang, Pigment & Resin Technology 43 (2013) 45–51, https://doi.org/10.1108/PRT-12-2012-0089.
[25] C.E. Johnson, P. Martin, K.A. Roberts, T. Trejos, R. Corzo, J.R. Almirall, A.M. Safer, J. Forensic Sci. 63 (2017) 66, https://doi.org/10.1111/1556-4029.13508.
[26] A. Braz, M. López-López, C. García-Ruiz, Forensic Sci. Int. 249 (2015) 92, https://doi.org/10.1016/j.forsciint.2015.01.023.
[27] M.N. Mohamad Asri, R. Verma, N.A. Mahat, N.A.M. Nor, W.N.S. Mat Desa, D. Ismail, Chemom. Intell. Lab. Syst. (2022) 225, https://doi.org/10.1016/j.chemolab.2022.104557.
[28] J.M.D.O.B. Brandão, N.S.M. Almeida, P.V.M. Dixini, C.H.A. Baier, H.P. Dias, J.F. P. Bassane, H.S. França, S.R.C. Silva, G.M.F.V. Aquije, W. Romão, Anal. Methods 8 (2015) 771, https://doi.org/10.1039/c5ay03128a.
[29] M.N.M. Asri, N.F. Nestrgan, N.A.M. Nor, R. Verma, Microchem. J. (2021) 165, https://doi.org/10.1016/j.microc.2021.106136.
[30] P. Papaspyridakou, P. Giannoutsou, M.G. Orkoula, Biosensors (Basel) 13 (2023) 135, 10.3390/bios13010135 (DOI:10.3390/bios13010135).
[31] S. Sharma, D. Garg, R. Chophi, R. Singh, Forensic Chem. 26 (2021) 100377, https://doi.org/10.1016/j.forc.2021.100377.
[32] S. Purba, M.K. Gupta, R.R. Gupta, Annals Romanian Soc. Cell Biol. 25 (6) (2021) 5794–5801.
[33] J. Gould, S. Clement, B. Crouch, R.S.P. King, Sci. Justice 63 (2023) 456–467, https://doi.org/10.1016/j.scijus.2023.04.016.
[34] R. Kaur, K. Saini, N.C. Sood, Sci. Justice 53 (2013) 212–219, https://doi.org/10.1016/j.scijus.2012.10.001.
[35] R. Glover, A. Furlought, P. Jasra, S.K. Jasra, J Emerging Forensic Sci Res 1 (2016) 67–86.
[36] V.A.G.D. Silva, M. Talhavini, J.J. Zacca, B.R. Trindade, J.W.B. Braga, J. Braz. Chem. Soc. (2014), https://doi.org/10.5935/0103-5053.20140140.
[37] Q. Sun, Y. Luo, Q. Zhang, X. Yang, C. Xu, J. Forensic Sci. 61 (2016) 1116, https://doi.org/10.1111/1556-4029.13067.
[38] G. Sauzier, J. Mcginn, T. Trubshoe, S.W. Lewis, Forensic Sci. Int. Rep. (2019) 1, https://doi.org/10.1016/j.fsir.2019.100021.
[39] Q. Sun, Y. Luo, X. Yang, P. Xiang, M. Shen, Forensic Sci. Int. 261 (2016) 71–81, https://doi.org/10.1016/j.forsciint.2016.01.038.
[40] B. De Carvalho, C. Mariaa, R. Ortiz, D. Reis Scorsatto, Z. Amanda, L.R. Pereira, F. M. Flores, V.B. Gontijo, C.M. Bello De Carvalho, C.M. Bello, FSAR (2018) 2, https://doi.org/10.31031/fsar.2018.02.000537.
[41] V. Tibljas, S. Francese, M. Da Costa Abreu, R. Bradshaw, Analyst 150 (2025) 2322–2335, https://doi.org/10.1039/D5AN00217F.
[42] P. Buzzini, E. Suzuki, J. Raman Spectrosc. 47 (2016) 16–27, https://doi.org/10.1002/jrs.4818.
[43] L. Heudt, D. Debois, T.A. Zimmerman, L. Köhler, F. Bano, F. Partouche, A. Duwez, B. Gilbert, E. De Pauw, Forensic Sci. Int. 219 (2012) 64–75, https://doi.org/10.1016/j.forsciint.2011.12.001.
[44] E. Pigorsch, J. Raman Spectrosc. 52 (2021) 78–84, https://doi.org/10.1002/jrs.5877.
[45] C. Krafft, E. Pigorsch, B. Weber, F. Ott, S. Brennecke, G.E. Krammer, R. Salzer, Vib. Spectrosc. 43 (2007) 49–52, https://doi.org/10.1016/j.vibspec.2006.06.009.
[46] M. Manso, S. Pessanha, M. Guerra, U. Reinholz, C. Afonso, M. Radtke, H. Lourenço, M. Carvalho, A. Guilherme Buzanich, Biol. Trace Elem. Res. (2019) 187, https://doi.org/10.1007/s12011-018-1406-y.
[47] M. Littler, Whisky Fraudsters Defeated By Invisible Molecular Fingerprints In Bottle Seals, https://www.forbes.com/sites/marklittler/2025/02/27/whisky-fraudsters-defeated-by-invisible-molecular-fingerprints-in-bottle-seals/, 2025.
[48] B.W. Blunden, J.W. Birkenshaw, in: R.H. Leach, C. Armstrong, J.F. Brown, M. J. Mackenzie, L. Randall, H.G. Smith (Eds.), The Printing Ink Manual, Springer US, Boston, MA, 1988, pp. 10–68.
[49] A.R. Buchberger, K. DeLaney, J. Johnson, L. Li, Anal. Chem. 90 (2018) 240–265, https://doi.org/10.1021/acs.analchem.7b04733.